Journal of Food Bioactives
International Society for Nutraceuticals and Functional Foods
Original Research
J. Food Bioact. 2025;000:000–000

# Anti-inflammatory effects of benzotropolone derivatives

Alexander Gosslau[a*], Shiming Li[b], Emmanuel Zachariah[c] and Chi-Tang Ho[d]

[a]Department of Science (Biology), City University of New York, BMCC, 199 Chambers Street, New York, NY 10007, USA
[b]College College of Biology and Agricultural Resources, Huanggang Normal University, Huanggang 438000, China
[c]OncoPath Genomics, Monmouth Junction, 7 Deer Park Drive, New Jersey 08852, USA
[d]Department of Food Science, Rutgers University, 65 Dudley Road, New Brunswick, New Jersey 08901-8520
[*]**Corresponding author:** Alexander Gosslau, Department of Science (Biology), City University of New York, BMCC, 199 Chambers Street, New York, NY 10007, USA. Tel: +1 212 2201305, Fax: +1 212 7487471, E-mail: agosslau@bmcc.cuny.edu
**DOI:** 10.26599/JFB.20xx.000xx
**Received:** September 02, 2025; **Revised received & accepted:** September 11, 2025
**Citation:** Gosslau, A., Li, S., Zachariah, E., and Ho, C.-T. (2025). Anti-inflammatory effects of benzotropolone derivatives. J. Food Bioact. 000: 000–000.

## Abstract

Therapeutic effects of black tea theaflavines (TFs) containing the benzotropolone (BZ) core structure of polyphenols are well established. In our study, we synthesized nine different BZ derivatives and tested them for anti-proliferative and anti-inflammatory bioactivities employing cell-based and *in vivo* models for inflammation. Three low molecular weight derivatives such as the natural-derived purpurogallin (BZ-5), 3, 4, 6-trihydroxy-5*H*-benzo[7]-annulen-5-one (BZ-6) and 3,4,6-trihydroxy-5-oxo-5H-benzo[7]annulen-1-yl)acrylic acid (BZ-7) showed strong anti-inflammatory effects. TaqMan qPCR demonstrated a prominent downregulation of *COX-2*, *TNF-α*, *ICAM-1*, *IL-1ß* and *IL-8*. Intriguingly, the new described compound BZ-7 showed strongest anti-inflammatory effects and only mild toxicity as compared to the others. Structure-activity relationship analysis revealed that placement of functional groups around the benzotropolone core moiety strongly affected anti-proliferative and anti-inflammatory bioactivities. Further analysis of BZ-6 representing the benzotropolone core moiety showed a significant down-regulation of *COX-2* in colonic carcinoma cells (Caco-2). Strong anti-inflammatory effects correlated in a mouse edema model where BZ-6 gave comparable effects to ibuprofen. In summary, our results indicate an inhibitory interaction of the BZ core moiety with cellular targets of inflammatory pathways as potential executioner of theaflavins through biotransformation. Thus, specific benzotropolones might be good candidate compounds with a therapeutic potential against diseases associated with chronic inflammation.

**Keywords**: Benzotropolones; Purpurogallin; Theaflavins; Black tea; Inflammation.

## 1. Introduction

Tea derived from leaves of *Camellia sinensis* is the most consumed beverage in the world only second to water. Teas are usually divided in three major groups such as green tea, oolong tea and black tea which differ in the degree of fermentation and consumption (Du et al., 2025; Ho et al., 2008; Li et al., 2013; Samanta, 2022; Sang et al., 2011). Whereas green tea is unfermented with a consumption of approximately 20% worldwide, leaves of oolong tea are semi-fermented and consumed around 2%. Black tea with the highest degree of fermentation has a consumption of around 78%. The different types of tea contain a distinct composition of diverse polyphenols such as catechins, theaflavins and thearubigins. During the fermentation process catechins are converted to polymeric polyphenols mainly into theaflavins and thearubigens which appear in high amounts in black tea. The formation of black tea polyphenols during fermentation involves the two steps of oxidation and polymerization. In the first reaction green tea catechins, mainly EGC and EGCG are partially oxidized to quinones by enzymatic catalysis of polyphenol oxidase (PPO) and peroxidase (POD) both naturally existing enzymes in fresh tea leaves. The second polym-

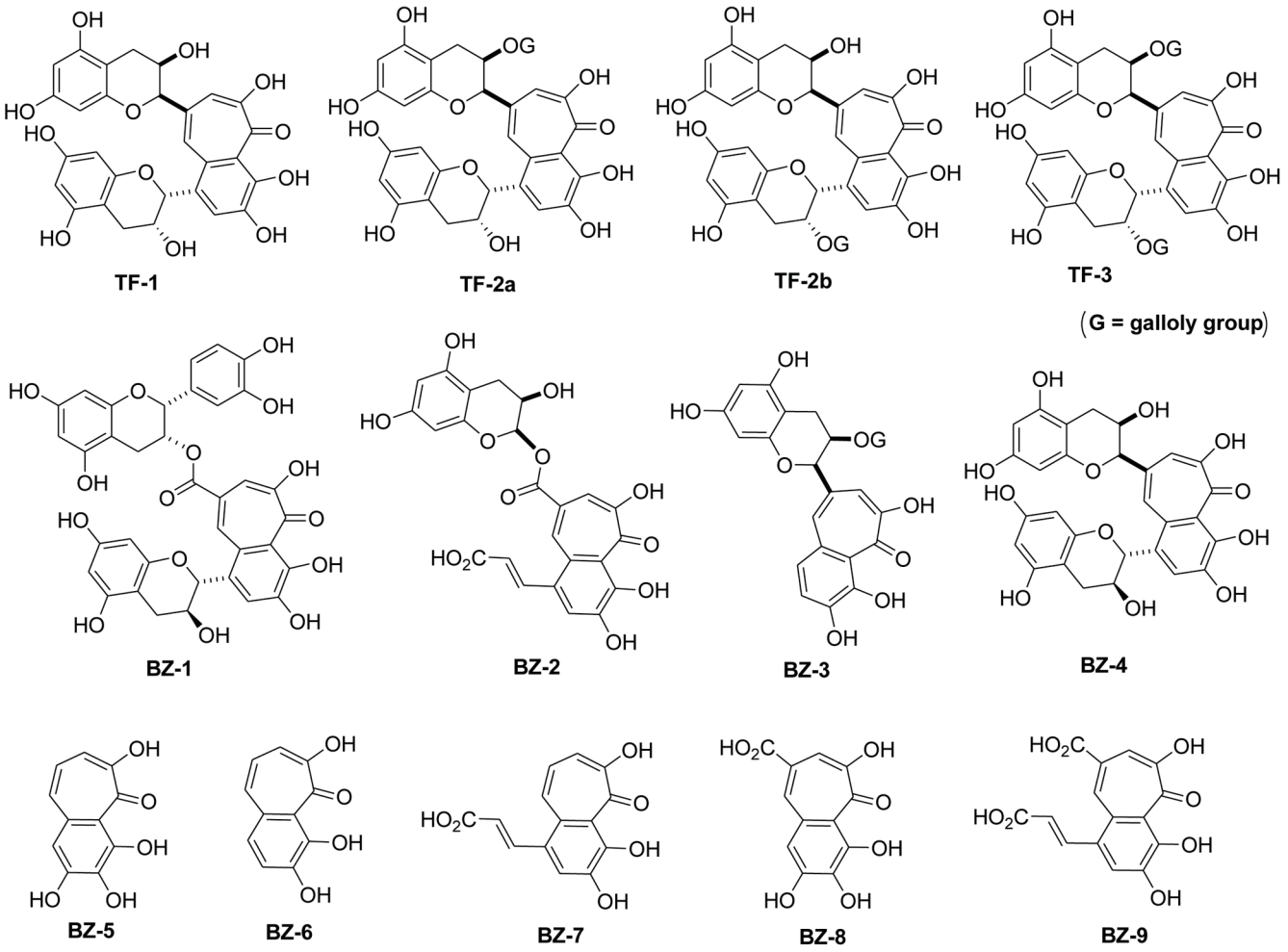


**Figure 1. Structure of benzotropolone derivatives.** Structures of the nine different benzotropolone derivatives (BZ-1 to BZ-9) are illustrated. For comparison, the four theaflavin isomers such as theaflavin (TF-1), theaflavin-3-*O*-gallate (TF-2), theaflavin-3′-*O*-gallate (TF-2′) and theaflavin-3,3′-*O*-*O*-digallate (TF-3) with the benzotropolone moiety as their core structure are also shown.

erization step involves a nucleophilic addition reaction of the resulting gallocatechin quinones to catechin quinones, followed by further oxidation by oxygen or hydrogen peroxide. Elimination of carbon dioxide and rearrangement then complete the synthesis of the benzotropolone structure, the core moiety of theaflavins (Du et al., 2025; He, 2017; Li et al., 2013; Samanta, 2022; Sang et al., 2011). Although accounting for only for 3 - 6% of the dry weight, health beneficial effects of black tea are mainly attributed to the group of theaflavins. Four different isoforms such as theaflavin (TF-1), theaflavin-3-*O*-gallate (TF-2a), theaflavin-3′-*O*-gallate (TF-2b) and theaflavin-3,3′-*O*-*O*-digallate (TF-3) (see Figure 1 for structures) have been described (Du et al., 2025; He, 2017; Li et al., 2013; Samanta, 2022; Sang et al., 2011). All theaflavins contain the benzotropolone core structure from the reaction of a catechol and pyrogallol during the polymerization reaction. In addition, several thearubigens contain one or more benzotropolone moieties as core structures in their molecules (Drynan et al., 2010; Gosslau et al., 2018; Li et al., 2013; Sang et al., 2011; Tanaka and Matsuo, 2020). It is the benzotropolone moiety which results in dark orange to dark brown color characteristic for black tea (Du et al., 2025; Ho et al., 2008; Samanta, 2022; Sang et al., 2011).

It is widely accepted that damaging effects of chronic inflammation are a major contributor to the development of numerous diseases. Inflammation is initiated by the activation of a variety of genes such as cyclooxygenase-2 (*COX-2*), tumor necrosis factor-*α* *(TNF-α)*, intracellular adhesion molecule-1 (*ICAM-1*), interleukin-1β (*IL-1β*) and interleukin-*8* (*IL-8*) as important mediators of the inflammatory cascade (Furman et al., 2019; Gosslau et al., 2011b; Robbins et al., 2010; van de Vyver, 2023). Activation of the transcription factor NFκB plays a central role in the induction of many of these but also other inflammatory genes. Some of them are further activating NFκB (e.g. *TNF-α* and *IL-1β*) through positive feedback mechanisms (Furman et al., 2019; Ghosh and Hayden, 2008; Robbins et al., 2010; van de Vyver, 2023). In addition, COX-2 and ICAM-1 are increasing the inflammatory cascade through vasodilation and chemotaxis of leukocytes triggered by the generation of different prostaglandins or other chemoattractants. Inflammation is characterized by phagocytosis and intracellular degradation of ingested material mediated through lysosomal enzymes and oxidative burst by neutrophils and macrophages (Chaudhary et al., 2023; Davies, 1995; Maldonado et al., 2023). In enzymatic reactions electrophilic species such as reactive oxygen

species (ROS) and reactive nitrogen species (RNS) are generated. In contrast to acute inflammation as beneficial part of the innate immune response, chronic inflammation is characterized by prolonged duration caused by persistent infections, immune-mediated inflammatory diseases, or prolonged exposure to toxic reagents. An important event in chronic inflammation is the differentiation of monocytes to macrophages. Macrophages activate *ICAM-1*, *COX-2*, several cytokines (e.g. TNF-α and IL-1β) and chemokines (e.g. IL-8) to perpetuate the inflammatory response (Furman et al., 2019; Gosslau et al., 2011b; Ley, 2001; Robbins et al., 2010; van de Vyver, 2023). Electrophilic species and proteolytic metalloproteinases then lead to accumulation of cell damage and tissue destruction during severe chronic inflammation. Thus, these damaging effects of chronic inflammation represent a major underlying cause of various degenerative diseases including cardiovascular, Alzheimer's, diabetes, rheumatoid arthritis, diabetes and cancer (Aggarwal et al., 2012; Calle and Fernandez, 2012; Furman et al., 2019; Ley, 2001; Robbins et al., 2010; van de Vyver, 2023).

It is generally believed that the health-promoting effects of black tea are based on anti-oxidant, anti-inflammatory and pro-apoptotic activities of theaflavins as their main underlying mechanisms (Du et al., 2025; Gosslau et al., 2018; Li et al., 2013; Samanta, 2022; Sang et al., 2011). Strong anti-oxidative effects of the three theaflavin isoforms have been described, reflected by prevention of pro-carcinogenic lipid peroxidation, lipoprotein oxidation, and DNA damage and mutation (Du et al, 2025; Gosslau et al., 2011a; Wu et al., 2016). According to their antioxidative activity prominent anti-inflammatory effects for TF-1, TF-2 and TF-3 have been described (Du et al., 2025; Gosslau et al., 2011a; He, 2017; Li et al., 2013; Samanta, 2022; Sang et al., 2011). Attenuation of key inflammatory cascade genes by theaflavins have been shown to target the NFκB signaling pathway (Du et al., 2025; Gosslau et al., 2011a; Samanta, 2022). In accordance to its anti-inflammatory and pro-apoptotic effects several studies demonstrated effects of black tea against diseases related to chronic inflammation such as cardiovascular, gastrointestinal, neurological and immunological disorders, diabetes, rheumatoid arthritis and different cancers (Du et al., 2025; He, 2017; Li et al., 2013; Samanta, 2022; Sang et al., 2011). A mystery in tea research has been the discrepancy between the well-established bioactivity of high molecular weight theaflavins on the one hand and poor bioavailability on the other (Li et al., 2025; Sang et al., 2011; Shi et al., 2022). Recently, we discussed a generation of secondary metabolites containing the benzotropolone structure formed by means of biotransformation through gut microbiota as possible candidates to explain the missing link (Gosslau et al., 2018).

Strong anti-oxidative and anti-inflammatory effects of the natural occurring benzotropolone-containing compound purpurogallin have been demonstrated in numerous studies (Chang et al., 2014; Kim et al., 2011; Park et al., 2013; Prasad et al., 1994; Sang et al., 2004; Wu et al., 1996; Zeng and Wu, 1992). Bioactivity against inflammation appears to affect NFκB signaling on level of iKK preventing iκB degradation thus leading to a suppression of NFκB activity (Park et al., 2013). The anti-inflammatory properties are in correspondence to effects of purpurogallin against cancer (Abou-Karam and Shier, 1999; Chakrabarty et al., 2013; Watanabe et al., 2009) but also to cardio- and hepatoprotective effects (Wu et al., 1994; Wu et al., 1991; Wu et al., 1996). In addition, proapoptotic effects for purpurogallin as another underlying pathway leading to anti-proliferative and anti-cancer effects have been reported (Kitada et al., 2003). There exist only few studies on the bioactivity of other benzotropolone derivatives. In 2004, Sang and coworkers performed a comparative structure-activity relationship (SAR) analysis of eighteen benzotropolone derivatives by the use of three different cancer cell lines. They found the benzotropolone moiety to be essential for anti-inflammatory activities and cytotoxic effects (Sang et al., 2004).

In our current study, we prepared nine different benzotropolone derivatives for a relationship analysis between molecular structure and biological activity on viability and inflammation using a human cell-based model. BZ-6 representing the benzotropolone core molecule was further tested in a paw edema *in vivo* mouse model.

## 2. Materials and methods

### 2.1. Materials and chemicals

Dulbecco's modified Eagle's medium (DMEM), Eagle's minimum essential medium (EMEM), RPMI-1640 medium, and fetal bovine serum (FBS) were obtained from Gibco BRL (Gaithersburg, MD). Cell culture flasks, dishes, and 24-well plates were from Falcon (Becton-Dickinson, Franklin Lakes, NJ). For RNA isolation, RNeasy™ Total RNA Kit (Qiagen, Chatsworth, CA) was used. Oligo-dT, dNTPs, Superscript™ II reverse transcriptase were purchased from Invitrogen, Life Technologies (Grand Island, NY). *Taq*Man qPCR probes, primers and master mix were from Applied Biosystems, Life Technologies (Grand Island, NY). Catechol, pyrogallol, gallic acid, (+)-catechin, (−)-epicatechin (EC), (−)-epigallocatechin (EGC), (−)-epicatechin gallate (ECG), and (−)-epigallocatechin gallate (EGCG), horseradish peroxidase, hydrogen peroxide ($H_2O_2$), and other chemicals were purchased from Sigma (St. Louis, MO).

### 2.2. Preparation of benzotropolones derivatives

Nine different benzotropolone derivatives were synthesized with structures illustrated in Figure 1 and respective molecular weights as indicated in brackets: BZ-1 (Neotheaflavate B, MW 700.61), BZ-2 (3,4,6-trihydroxy-5-oxo-8-(((2*R*,3*R*)-3,5,7-trihydroxy-3,4-dihydro-2H-chromen-2-yloxy)carbonyl)-5H-benzo[7]annulen-1-yl) acrylic acid, MW 580.45), BZ-3 (*(2R,3R)*-5,7-dihydroxy-2-((5E,7E)-1,2,8-trihydroxy-9-oxo-9H-benzo[7]annulen-6-yl)-3,4-dihydro-2H-chromen-3-yl 3,4,5-trihydroxybenzoate, MW 566.51), BZ-4 (Neotheaflavin, MW 564.50), BZ-5 (Purpurogallin, MW 220.18), BZ-6 (3, 4, 6-trihydroxy-5*H*-benzo[7]-annulen-5-one, MW 204.18), BZ-7 (3,4,6-trihydroxy-5-oxo-5H-benzo[7]annulen-1-yl)acrylic acid (, MW 248.19), BZ-8 (1,2,8-trihydroxy-9-oxo-9H-benzo[7]annulene-6-carboxylic acid, MW 248.19), and BZ-9 (4-(2-carboxyvinyl)-1,2,8-trihydroxy-9-oxo-9H-benzo[7]annulene-6-carboxylic acid, MW 292.20). The synthetic procedure of the nine benzotropolone compounds was followed Sang's procedure (Ho et al., 2006; Sang et al., 2004). Specifically, BZ-1 (Neotheaflavin B) was synthesized from catechin and EGCG; BZ-2 from caffeic acid and EGCG; BZ-3 from catechol and EGCG; BZ-4 (Neothealflavin) from catechin and EGC; BZ-5 (Purpurogallin) from pyrogallol; BZ-6 from catechol and pyrogallol; BZ-7 from caffeic acid and pyrogallol; BZ-8 from gallic acid and pyrogallol; and BZ-9 from gallic acid and caffeic acid. All the products after purification were characterized with HRMS and NMR and in accordance with reported data (Ho et al., 2006; Sang et al., 2004).

### 2.3. Cell culture and treatment

U-937 cells (CRL-1593.2, human histiocytic lymphoma), Caco-2 cells (HTB-37, human colorectal adenocarcinoma) and HepG2

(HB-8065, human hepatocellular carcinoma) were obtained from the American Type Culture Collection (Rockville, MD). All cell lines had low passage numbers (below 30) and cell growth and density were monitored routinely. Cells were either cultured in RPMI-1640 medium (for U-937 cells), Dulbecco's modified Eagle's medium (for Caco-2 cells) or Eagle's minimum essential medium (for HepG2 cells) with 10% FBS at 37°C in a humidified, 10% $CO_2$ atmosphere. Cells were subcultured in culture flasks (Falcon, Becton-Dickinson, Franklin Lakes, NJ) and passaged every 3 days. Before experiments, cells were seeded in 60 mm culture dishes or 24-well plates (Falcon, Becton-Dickinson, Franklin Lakes, NJ) as indicated for the different assays. Different benzotropolone derivatives were applied directly to the medium to achieve final concentrations as indicated.

### 2.4. MTT cell proliferation assay

Proliferation of U-937 monocytes was measured by the MTT (3(4,5-dimethylthiazol-2-yl)-2,5-diphenyl-tetrazolium-bromide) method after treatment in 24-well plates at different concentrations for 3 h, 24 h, or 5 days. The MTT-assay measures mitochondrial activity based on conversion of the tetrazolium salt MTT to blue formazan by mitochondrial dehydrogenase activity (Berg et al., 1990). Color development was documented by a scanner (UMAX, Astra 2200) and absorbance determined spectrophotometrically at 570 nm using a multi-well plate spectrophotometer (Infinite M200, Tecan, Maennedorf, Switzerland). Viability is given in percent of the control value (e.g. DMSO controls) and corresponding $IC_{50}$ values (e.g. 50% of growth inhibition) are indicated in the Results section. In view of the concern that MTT may yield false-positive results for certain cell types when treated with polyphenols (Bernhard et al., 2003), proliferation data were verified by trypan blue cell counting. For some benzotropolone derivatives a 24-hr viability test using human hepatocellular carcinoma cells (HepG2) was performed.

### 2.5. Human cell-based models for inflammation

For analysis of anti-inflammatory potential, we used U-937 cells as a monocyte-macrophage differentiation model for nutrigenomic analysis (Gosslau et al., 2011b). Briefly, U-937 cells were treated by the inflammatory stimulant 12-O-tetradecanoylphorbol-13-acetate (TPA; 20nM) for 3h either alone or in combination with the benzotropolone derivatives. The expression of a subset of inflammatory surrogate genes during differentiation to macrophages is then used as measure for anti-inflammatory bioactivity (Forsbeck et al., 1985; Gosslau et al., 2011b). We employed six inflammatory surrogate genes (*COX-2*, *TNF-α*, *ICAM-1*, *NFκB*, *IL-1β*, and *IL-8*) which had been previously selected and validated throughout various cell-based, animal and clinical studies by whole genome Affymetrix microarray, focused Oligo microarray and TaqMan qPCR analysis (Gosslau et al., 2014; Gosslau et al., 2011a; Gosslau et al., 2011b; Gosslau et al., 2008). Glyceraldehyde-3-phosphate dehydrogenase (GAPDH) as house-keeping gene was used as internal control. Gene expression analysis was performed by either RT-PCR or *Taq*Man qPCR analysis. In addition to U-937 cells, we used human colon cancer cells (Caco-2) for nutrigenomic analysis. Previously, we observed an upregulation of a variety of inflammatory genes by TPA in Caco-2 cells (Gosslau et al., 2011a).

### 2.6. Mouse paw edema model

The carrageenan-induced mouse hind paw edema model was used for determination of anti-inflammatory activity for BZ-6 by measuring the degree of edema formation (Morris, 2003). Male albino mice (6 weeks old) were group housed (6 per cage) and fed standard mouse chow and tap water *ad libitum*. All animal experiments were approved by the Ethics Committee for Animal Experiments of Rutgers University and were performed in accordance with the Guideline for Animal Experiments of the laboratories (protocol No. 87-115). For experiments, mice were grouped in three different cohorts (six animals per treatment group and time point) and treated by a single oral dose of BZ-6 (250 mg/kg) and compared to the vehicle control (tocopherol-stripped corn-oil). The concentration was chosen based on earlier studies analyzing the effects of theaflavin-2 or a theaflavin-enriched black tea extract, respectively (Gosslau et al., 2011a; Gosslau et al., 2011b). As positive control we included ibuprofen (100 mg/kg) demonstrated to have strong anti-inflammatory effects in the paw edema model in comparable studies (Gosslau et al., 2014; Moilanen et al., 2012). 1 h after treatment, all groups received an injection of 0.1 mL of carrageenan (1% in water) into the plantar side of the right hind paw of the mice. The mice were then euthanized 1, 2, 4, and 8 h after carrageenan injection and hind paws taken. The degree of swelling was determined by paw volume displacement measured by a digital hydroplethysmometer. Results are expressed as area under the curve (AUC) units or volume of hind paw (mL) at indicated times, respectively.

### 2.7. TaqMan qPCR analysis

After cell treatment as described under 2.5., total RNA was isolated using the QIAcube from Qiagen (Chatsworth, CA) according to manufacturer's protocols. Total RNA was then reverse transcribed using standard protocols and reagents from Invitrogen, Life Technologies (Grand Island, NY). *Taq*Man qPCR was run on the Roche 480 Lightcycler for 50 cycles with concentrations ranging from 100 ng to 0.01 ng for the standard curve. Gene expression of *COX-2* (Hs01573471_m1), *TNF-α* (Hs00174128_m1), *ICAM-1* (Hs99999152_m1), *NFκB* (Hs00153294_m1), *IL-1β* (Hs00174097_m1), *IL-8* (Hs00174103_m1), and *GAPDH* (Hs99999905_m1) was analyzed using the probes, primers and master mix from Applied Biosystems, Life Technologies (Grand Island, NY; for details see the Assay IDs as indicated above in brackets next to the respective genes). After normalization to *GAPDH*, gene expression was calculated according to the delta-delta CT method as ratio of the mean experimental channel (TPA + BZ) to the mean control channel (TPA alone). Besides ratios, degree of gene expression is also expressed as "inflammatory index" which was calculated as Log2 values of the ratios as described below.

### 2.8. Reverse transcription-polymerase chain reaction (RT-PCR)

For analysis of *COX-2* expression in Caco-cells but also for routine purposes, traditional RT-PCR analysis employing gel electrophoresis and semi-quantitative densitometry was used for *COX-2* and *GAPDH* as inflammatory surrogate or house-keeping gene, respectively. After treatment for 3h, RNA was isolated, and reverse transcribed into cDNA as described above. For PCR amplification, gene specific primers were used for *COX-2* (sense, 5′-ttcaaatgagattgtgggaaaat-3′; antisense, 5′-agatcatctctgcctgagtatctt-3′) and *GAPDH* (sense: 5′-tgaagctcggagtcaacggatttg-3′; antisense: 5′-catgtgggccatgaggtccaccac-3′). PCR conditions were chosen to ensure that the yield of the amplified product was linear with respect to the amount of input cDNA. PCR products were analyzed by elec-

trophoresis on a 1% agarose gel and visualized with ethidium bromide staining. *COX-2* and *GAPDH* expression was quantified by densitometry using the Image J software (NIH, Bethesda, MD). *COX-2* expression was then normalized to *GAPDH* and expressed as ratio of the mean experimental channel (TPA + BZ) to the mean control channel (TPA alone) or as "inflammatory index" as described below.

### 2.9. Oligo-microarray analysis

U-937 cells were treated with TPA (20nM) either alone or in combination with BZ-6 (50 µg/ml) for 3h. After RNA isolation and reverse transcription, expression of *COX-2*, *$LTA_4$ hydrolase*, *TNF-α, TNF-α receptor*, *iNOS*, *ICAM-1*, *IL-1β*, *IL-8*, *IL-15*, *IL-18*, *NFκB*, *c-Jun*, *c-Fos*, and *p53* was analyzed by a proprietary Oligo microarray. As housekeeping genes, ATP synthase mitochondrial complex subunit b1 (*ATP5F1*), eukaryotic translation initiation factor 4A1 (*EIF4A1*), myristoylated alanine-rich protein kinase C substrate (*MARCKS*), phosphoglycerate kinase 1 (*PGK1*), proteasome subunit beta type 5 (*PSMB5*), and glutaminyl-tRNA synthetase (*QARS*) were employed. Gene expression is expressed as "fold gene expression" by cluster analysis (blue indicate anti-inflammatory effects, red cluster indicate inflammatory effects) after calculating the ratio of mean experimental channel (TPA + BZ-6) to the mean control channel (TPA alone) normalized to spike-in controls (e.g. alien DNA (Stratagene) labeled as C-1 to C-5).

### 2.10. Inflammatory Index

The inflammatory index indicates either pro- or anti-inflammatory effects. It is based on the delta-delta CT method indicating the ratio between experimental (TPA plus BZs) and control channel (TPA alone) normalized to the expression of housekeeping genes. Ratiometric numbers (indicated as fold gene expression) are then converted into log 2 base values (ratios below 1 transform into negative numbers) and expressed as inflammatory index. Based on the inflammatory index, anti-inflammatory potential is indicated by negative numbers, whereas positive index numbers are indicative for pro-inflammatory effects.

### 2.11. Statistics

Results are presented as means ± standard deviation (SD) of at least three independent experiments unless otherwise indicated. Statistical comparisons of data were performed using the Student's *t*-test or analysis of variance (ANOVA) as indicated.

## 3. Results

### 3.1. Effects of different BZs on viability of U-937 cells

First, long-term effects of seven benzotropolone derivatives on cell viability using the MTT-method were analyzed. After treating U-937 cells for 5 days with different concentrations of BZs, effects on cell viability were analyzed and expressed in percent as compared to untreated controls (Figure 2a). We observed different anti-proliferative activities of BZs as indicated by different $IC_{50}$ values (e.g. half-maximal inhibition of viability). BZ-6 with the lowest molecular weight (MW 204.18) showed strongest effects on cell viability ($IC_{50}$ around 5 µg/mL or 24 µM, respectively). Although we did not include BZ-1 and BZ-4 in our studies we observed that higher molecular weight derivatives such as BZ-2 (MW 580.45) and BZ-3 (MW 566.51) showed lesser effects on cell viability as indicated by $IC_{50}$ values of around 50 µg/mL for BZ-2 (86 µM) or 40 µg/mL for BZ-3 (71 µM), respectively. As judged by $IC_{50}$ molarity values other low molecular derivatives such as BZ-5, BZ-7, BZ-8, and BZ-9 showed even lesser anti-proliferative effects as compared to BZ-2 and BZ-3: BZ-5 (136 µM), BZ-7 (121 µM), BZ-8 (121 µM) and BZ-9 (240 µM).

Intriguingly, the comparison throughout low molecular weight derivatives (e.g. BZ-5 - BZ-9) revealed that placement of functional groups at different positions around the benzotropolone core structure affected cell viability. BZ-6 representing the benzotropolone core structure with only one ketone group and three hydroxyl groups (3, 4, 6-trihydroxy-5*H*-benzo[7]-annulen-5-one) exhibited strongest cytotoxicity with an $IC_{50}$ value of around 5 µg/mL (24 µM). Purpurogallin (BZ-5) with an additional hydroxyl group at C-2 showed significant lesser cytotoxicity ($IC_{50}$ of around 30 µg/mL; 136 µM). Similar $IC_{50}$ values were observed for BZ-7 and BZ-8 (both around 121 µM) which contain an additional carboxyl group at C-1 or C-8, respectively. BZ-9 with two additional carboxyl groups at C-1 and C-8 showed least cytotoxicity ($IC_{50}$ around 70 µg/mL; 240 µM) as compared to the other low molecular weight derivatives but also to the larger BZ-2 ($IC_{50}$ around 50 µg/mL; 86 µM) and BZ-3 ($IC_{50}$ around 40 µg/mL; 71 µM).

We then performed a more detailed dose response and kinetic analysis of three benzotropolone derivatives representing either a high molecular weight molecule showing low cytotoxicity (BZ-2) or low molecular weight derivatives showing strong (BZ-6) or low cytotoxicity (BZ-9) after 5 days of exposure, respectively (Figure 2a). Dose response analysis was performed in the range from 0.1 - 100 µg/mL after 3 h, 24 h, and 5 days of exposure (Figure 2b). As expected, we observed an increase in cytotoxicity in response to longer exposure times for BZ-2, BZ-6 and BZ-9. BZ-6 exhibited strongest cytotoxicity as indicated by $IC_{50}$ values of around 75 µg/mL (367 µM), 7.5 µg/mL (37 µM) or 5 µg/mL (24 µM) after 3 h, 24 h, and 5 days, respectively. Although we observed similar $IC_{50}$ values for BZ-2 (around 50 µg/mL) and BZ-9 (around 70 µg/mL) after 5 days due to the difference in molecular weight the $IC_{50}$ values calculated for molarity are different (e.g. 86 µM and 240 µM for BZ-2 or BZ-9, respectively). Interestingly, after 3h the toxicity profiles of BZ-2 and BZ-9 looked very similar (viability of more than 90% in response to 100 µg/mL) but we noted a difference in the profile after 24 h and 5 days of incubation. Whereas BZ-9 showed stronger cytotoxicity after 24 h as compared to BZ-2 ($IC_{50}$ of around 75 µg/mL and 100 µg/mL for BZ-9 or BZ-2, respectively), after 5 days the cytotoxic effects of BZ-2 (around 50 µg/mL) were stronger in comparison to BZ-9 (around 70 µg/mL).

In summary, our structure-activity relationship analysis did not reveal an apparent correlation between molecular size and anti-proliferative activities as indicated by $IC_{50}$ values after 5 days: derivatives with similar size showed either different (e.g. BZ-9 (240 µM), BZ-6 (24 µM), BZ-5 (136 µM)) or same activities (e.g. BZ-7 and BZ-8 (both around 121 µM)). Moreover, small derivatives (BZ-9; 240 µM) showed lesser effects as compared to high molecular derivatives (BZ-2 (86 µM) and BZ-3 (71 µM)).

### 3.2. Effects of different benzotropolone derivatives on expression of inflammatory genes in U-937

In the next set of experiments the bioactivity of the benzotropolone derivatives against inflammation was analyzed. Anti-inflammato-

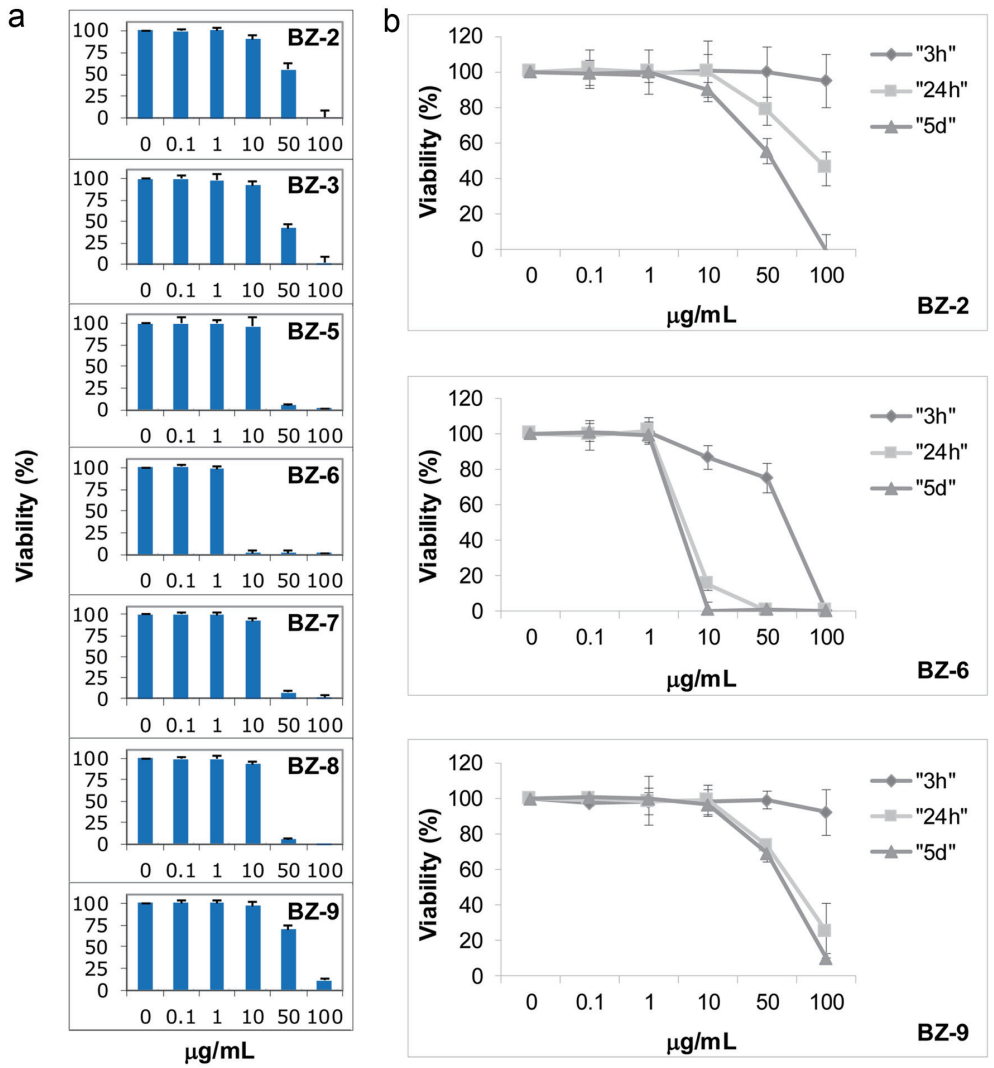


**Figure 2. Effects of benzotropolone derivatives on cell viability.** Human monocytes (U-937) were treated with different BZ derivatives at indicated concentrations and measured by the MTT assay. Mean values ± standard deviation of at least three independent experiments is shown. Cells were exposed to BZs either at different concentrations for 5 days (a) or different concentrations of BZ-2, BZ-6 and BZ-9 were incubated for 3 h, 24 h, or 5 days as indicated by different symbols (rhombus, square, and triangle), respectively (b).

ry effects of purpurogallin had been demonstrated in *in vitro* cell-based and *in vivo* animal experiments (Chang et al., 2014; Kim et al., 2011; Park et al., 2013). On the other hand, studies on other BZ derivatives are very limited and anti-inflammatory effects for only a few other derivatives have been shown (Sang et al., 2004). For initial screening, we chose cyclooxygenase-2 (*COX-2*) as inflammatory surrogate gene which had been tested throughout previous cell-based, animal and clinical studies, previously (Gosslau et al., 2011b; Gosslau et al., 2008; Smith et al., 2000). Figure 3a shows the expression of *COX-2* normalized to *GAPDH* for the nine benzotropolone derivatives (50 µg/mL) after 3 h either as the ratio of the mean experimental channel (TPA + BZ) to the mean control channel (TPA alone) indicated as "I" or as inflammatory indices (Log2 values of the ratio) indicated as "II", respectively, as described in the Materials and Methods section. Although BZ-6 showed some anti-proliferative effects in response to 50 µg/mL after 3h with a cell viability around 75% (Figure 2b) inhibitory effects on gene transcription are less likely since no changes in *GAPDH* expression were observed (data not shown). We observed a drastic decrease of TPA-induced *COX-2* expression for BZ-5 (ratio = 0.10; index = −3.38), BZ-6 (ratio = 0.15; index = −2.72) and BZ-7 (ratio = 0.10; index = −3.39) as compared to the TPA control (all with $P < 0.001$). In contrast, the other BZ derivatives did not affect COX-2 expression significantly. Whereas BZ-8 showed a slight suppression, BZ-1, BZ-2, BZ-3, BZ-4 and BZ-9 showed slight pro-inflammatory effects as indicated by ratios above 1 (I) or positive inflammatory indices (II), respectively, although in a non-significant range.

For a more in-depth analysis of effects against inflammation representative members of small BZ derivatives were selected which showed strong *COX-2* suppression (e.g. BZ-5, BZ-6 and BZ-7) in comparison with BZ-8 which did not affect *COX-2* expression. We extended our analysis to a subset of six inflammatory surrogate genes (*COX-2*, *TNF-α*, *ICAM-1*, *NFκB*, *IL-1β*, and *IL-8*) normalized to *GAPDH* by *Taq*Man qPCR illustrated as inflammatory indices (Figure 3b). As already observed by initial screening (Figure

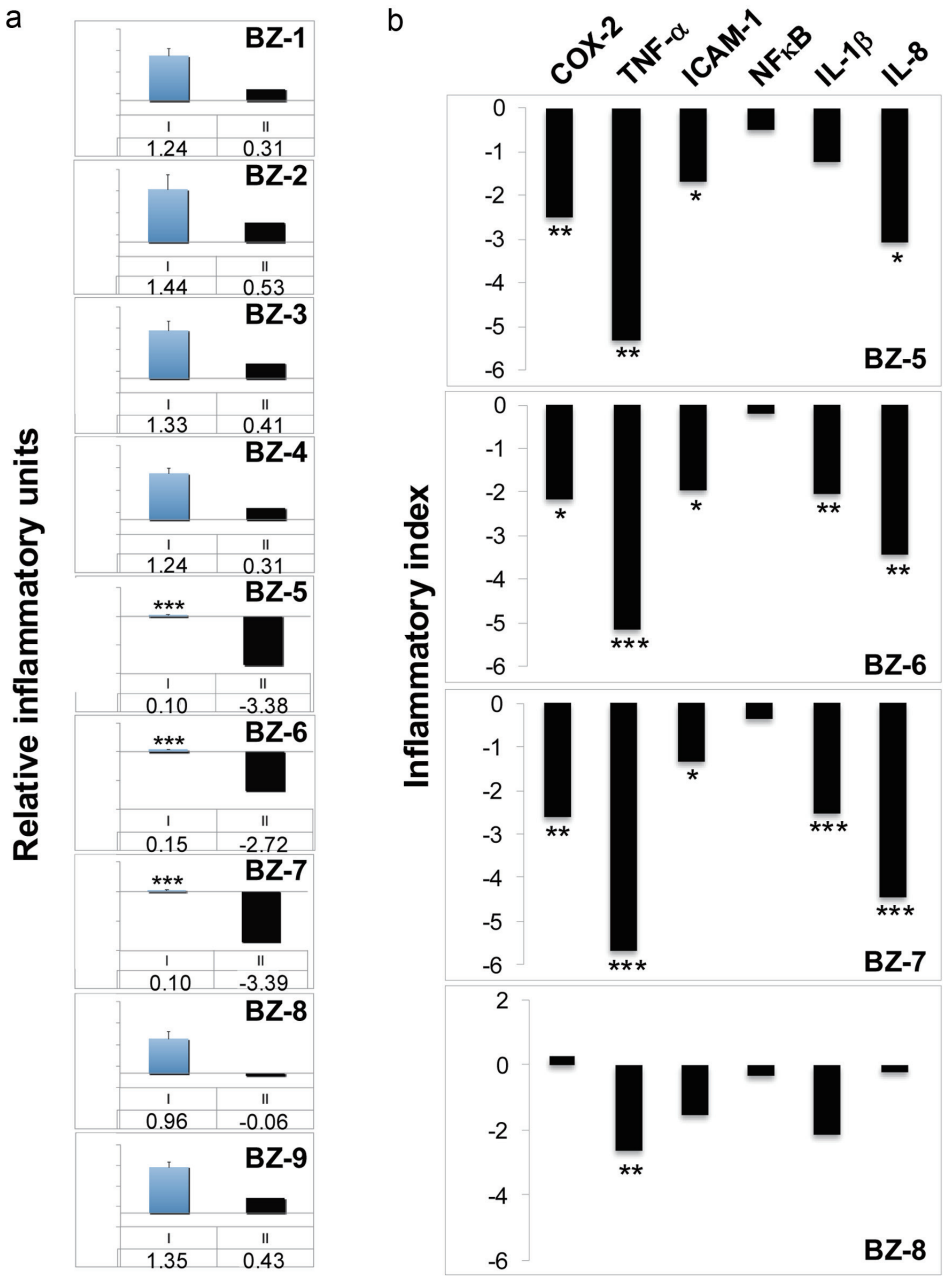


**Figure 3. Effects of benzotropolone derivatives on the expression of inflammatory genes.** Human monocytes (U-937) were treated with TPA (20nM) either alone or in combination with different BZs (50 µg/ml) for 3h. After RNA isolation and reverse transcription, expression of either *COX-2* (a) or (b), a panel of different inflammatory genes (*COX-2*, *TNF-α*, *ICAM-1*, *NFκB*, *IL-1β*, and *IL-8*) was analyzed by *Taq*Man qPCR analysis. The expression of glyceraldehyde-3-phosphate dehydrogenase (*GAPDH*) was used as internal control. After normalization to *GAPDH* according to the delta-delta CT method, gene expression is expressed as a ratio of the mean experimental channel (TPA + BZ) to the mean control channel (TPA alone). Ratios converted into Log2 values are expressed as inflammatory index as described in Materials and Methods. *, **, and *** indicate significant differences from the control group with $P < 0.05$, 0.01 or 0.001, respectively, as analyzed by the student's *t*-test of at least three independent experiments. (a) *COX-2* expression is either shown as mean ratios + standard deviation indicated by blue columns (I, mean value below) or as inflammatory indices indicated by black columns (II, inflammatory index below). (b) Inflammatory indices of *COX-2*, *TNF-α*, *ICAM-1*, NFκB, *IL-1β*, and *IL-8* are shown for BZ-5, BZ-6, BZ-7 and BZ-8 indicated by black columns.

3a), *COX-2* was strongly suppressed by BZ-5, BZ-6 and BZ-7 as demonstrated by negative indices ranging between -2 and -3. In correspondence to our initial screening, BZ-8 did not show major effects on *COX-2* expression and only *TNF-α* was significantly suppressed ($P < 0.01$). On the other hand, BZ-5, BZ-6 and BZ-7, consistent with a strong inhibition *of COX-2*, induced a prominent down-regulation of *TNF-α*, *ICAM-1*, *IL-1β*, and *IL-8*. Interestingly, we did not observe a downregulation of *IL-6* in response to all small BZ derivatives (data not shown). *NFκB* (e.g. the p65 subunit) did not show major changes in response to the four BZ derivatives

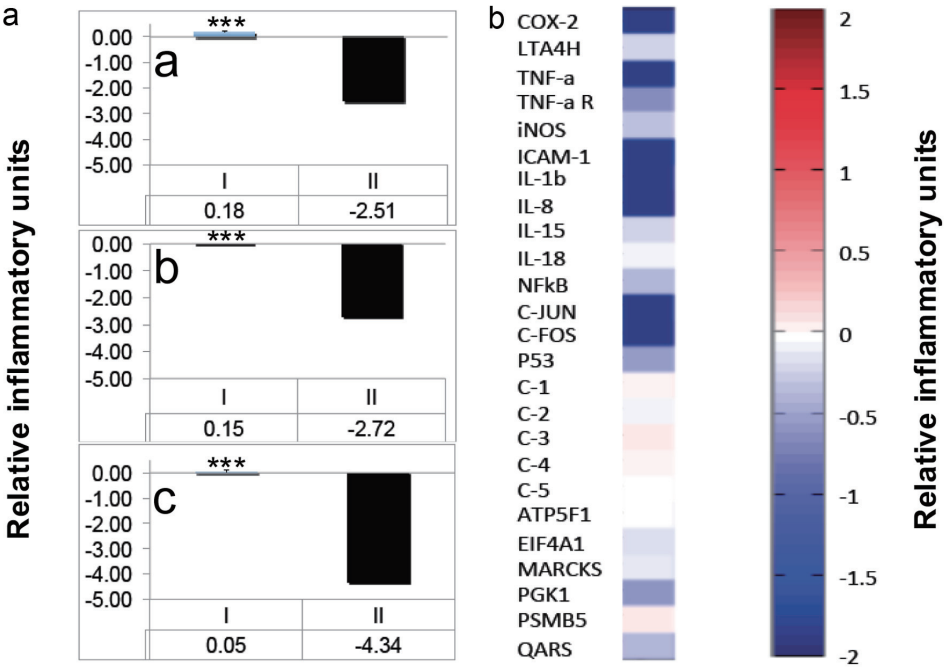


**Figure 4. Effects of BZ-6 in U-937 cells.** (a) Human monocytes (U-937) were treated with TPA (20nM) either alone or in combination with different concentrations of BZ-6 (25, 50 and 100 µg/ml) for 3h as indicated (a, b or c, respectively). After RNA isolation and reverse transcription, expression of *COX-2* was analyzed by *Taq*Man qPCR analysis. The expression of glyceraldehyde-3-phosphate dehydrogenase (*GAPDH*) was used as internal control. After normalization to *GAPDH*, gene expression was calculated as ratios (I) or inflammatory indices (II), respectively. *** indicate significant differences from the control group with $P < 0.001$ as analyzed by the student's *t*-test of at least three independent experiments. (b) U-937 cells were treated with TPA (20nM) either alone or in combination with BZ-6 (50 µg/ml) for 3h. After RNA isolation and reverse transcription, expression of *COX-2*, *$LTA_4$ hydrolase*, *TNF-α, TNF-α receptor*, *iNOS*, *ICAM-1*, *IL-1β*, *IL-8*, *IL-15*, *IL-18*, *NFκB*, *c-Jun*, *c-Fos*, and *p53* was analyzed by a proprietary Oligo microarray as described in Material and Methods. Artificial DNA sequences were used as control genes (C-1 - C-5) for normalization. As housekeeping genes, *ATP5F1*, *EIF4A1*, *MARCKS*, *PGK1*, *PSMB5*, and *QARS* were employed. Gene expression is shown as relative inflammatory units by cluster analysis. Upregulation is indicated by red colors, downregulation by blue colors, whereas no regulation is indicated by white colors. One set of representative data is shown of two independent experiments.

which correspond to a regulation majorly on posttranslational level (Baud and Karin, 2009; Ghosh and Hayden, 2008). By integrating all six genes (*COX-2*, *TNF-α*, *ICAM-1*, *NFκB*, *IL-1β*, *IL-8*) the average ratios were calculated as inflammatory indices: BZ-5, BZ-6 and BZ-7 showed strong bioactivities against inflammation as illustrated by relatively low indices of −1.99, −2.02 or 2.15, respectively. On the other hand, the anti-inflammatory effect of BZ-8 was much lesser as indicated by an inflammatory index of −0.98.

By integrating the data obtained by viability analysis (Figure 2) some features of structure-activity relationship between viability and inflammation can be derived for the tested benzotropolones: (i) As observed for cell viability there appear also no correlation between molecular size and anti-inflammatory activities: high molecular (e.g. BZ-1 to BZ-4) as well as low molecular benzotropolones (e.g. BZ-8, BZ-9) did not affect *COX-2* expression significantly. Among small derivatives strong anti-inflammatory effects were observed only for BZ-5, BZ-6, and BZ-7. A panel analysis throughout BZ-5 - BZ-8 confirmed strong anti-inflammatory bioactivities for BZ-5, BZ-6, and BZ-7 as compared to BZ-8. (ii) There appear also no simple relationship between bioactivities against proliferation and inflammation: derivatives showed either both strong anti-proliferative and anti-inflammatory activities (e.g. BZ-6), relative mild anti-proliferative but strong anti-inflammatory activities (e.g. BZ-5 and BZ-7), low anti-proliferative activity and no effects on *COX-2* expression (e.g. BZ-9) or relative strong anti-proliferative activities but no anti-inflammatory activities (e.g. BZ-2 and BZ-3). (iii) A comparison throughout low molecular derivatives demonstrated that placement of functional groups around the benzotropolone moiety are crucial for their anti-proliferative and anti-inflammatory activities: BZ-6 as the benzotropolone core structure with one ketone (at C-5) and three hydroxyl groups (at C-3, C-4, C-6) showed strong anti-proliferative and anti-inflammatory effects. The addition of either a hydroxyl (BZ-5) or carboxyl group (BZ-7) at C-2 or C-1, respectively, showed relative mild anti-proliferative but strong anti-inflammatory activities. On the other hand, an additional carboxyl group at C-8 (BZ-8) resulted in relative mild anti-proliferative as well as low anti-inflammatory activities. The derivative with two additional carboxyl groups at C-1 and C-8 showed lowest anti-proliferative and no anti-inflammatory activity as judged by *COX-2* analysis (BZ-9). These features, although preliminary, are in line with the notion that the underlying bioactivities of benzotropolones affecting cell viability and inflammation are different and due to specific interaction with cellular targets.

### 3.3. *Effects of BZ-6 on expression of inflammatory genes*

To gain more insights into the relationship between cytotoxicity and gene expression we chose BZ-6 representing the benzotropolone core moiety which showed strongest anti-proliferative bioactivity among our BZ derivatives as demonstrated by MTT-analysis (Figure 2) as well as strong anti-inflammatory bioactivity (Figure 3). The MTT method is considered to monitor early cytotoxic effects

based on mitochondrial dehydrogenase activity (Berg et al., 1990). Our kinetic experiments indicate strong damaging effects of BZ-6 on mitochondrial activity (0% viability) at 100 µg/mL after 3 h of exposure (Figure 2b). Surprisingly, we observed only a slight decrease in the expression of *GAPDH* when testing the effects of BZ-6 on TPA-induced *COX-2* expression at 100 µg/mL (data not shown). These results indicate that despite the loss of mitochondrial activity the impact of high concentrations of BZ-6 (e.g. 100 µg/mL) on gene expression machinery appear to be less prominent. Interestingly, a 24-hr MTT viability test showed similar $IC_{50}$ values in human liver cells (HepG2) in response to BZ-6 as compared to U-937 cells indicative that harmful conversion through cytochrome p450 or other systems is unlikely (data not shown). Figure 4a shows the impact of BZ-6 on *COX-2* expression normalized to *GAPDH* in response to 25, 50, and 100 µg/mL. We observed a decrease of *COX-2* expression in a dose-responsive manner (a-c) showing a strong inhibition of *COX-2* expression by BZ-6 at 25 µg/mL (122 µM) but even lower concentrations might be effective.

In further experiments, we analyzed the impact of BZ-6 (50 µg/mL) on additional inflammatory genes and analyzed TPA-induced gene expression by Oligonucleotide DNA microarray after 3 h (Figure 4b). As observed for *GAPDH*, other house-keeping genes such as *ATP5F1* (ATP synthase mitochondrial complex subunit b1) and *PSMB5* (proteasome subunit beta type 5) did not show significant changes. On the other hand, high concentrations of BZ-6 induced a down-regulation of other house-keeping genes such as *EIF4A1* (eukaryotic translation initiation factor 4A1), *MARCKS* (myristoylated alanine-rich protein kinase C substrate), *PGK1* (phosphoglycerate kinase 1), and *QARS* (glutaminyl-tRNA synthetase). As observed for COX-2 by Taq*Man* analysis (Figure 4a) the impact of BZ-6 on the expression of other inflammatory genes was relatively higher as compared to the housekeeping control genes as demonstrated by a strong down-regulation of *COX-2*, *TNF-α*, *ICAM-1*, *IL-1β* and *IL-8*. On the other hand, the regulation of *TNF-α R*, *iNOS*, *IL-15*, *IL-18*, *NFκB (p65)*, and *P53* in response to high concentrations of BZ-6 appear to be minor or not affected. Interestingly, although only for high concentrations, anti-inflammatory activity of BZ-6 - among other factors - might be based by decreased activity of AP-1 as indicated by decreased *C-JUN* and *C-FOS* expression.

### 3.4. Effects of BZ-6 on carrageenan-induced paw edema in mice and COX-2 expression in human Caco-2

Using a carrageenan-induced paw edema model, we investigated the effects of BZ-6 which showed strong anti-inflammatory potential as indicated by strong down-regulation of inflammatory surrogate genes as demonstrated in our cell-based model for inflammation (see 3.3 and 3.4). For experiments, mice were treated by BZ-6 (250 mg/kg) and compared to the vehicle control. Kinetic analysis (Figure 5a) showed that significant inhibitory effects of BZ-6 started as soon as 2 hours after carrageenan injection ($P < 0.05$). After 4 and 8 hours the inhibition of paw edema in response to BZ-6 was even stronger as compared to the vehicle control ($P < 0.001$). In another set of experiments, we included ibuprofen (100 mg/kg) as positive control in our carrageenan-induced paw edema model. Strong anti-inflammatory effects of ibuprofen in the paw edema model have been demonstrated previously (Gosslau et al., 2014; Moilanen et al., 2012). In correspondence to our kinetic analysis (Figure 5a), 8 hours after carrageenan injection a strong reduction of paw edema by BZ-6 as compared to the control group was observed (Figure 5b). Importantly, BZ-6 showed even slightly stronger anti-inflammatory effects ($P < 0.01$) as compared to ibuprofen ($P < 0.05$).

Many studies demonstrate a strong connection between chronic intestinal inflammation and the development of colorectal cancer (Aggarwal et al., 2012; Coussens and Werb, 2002; Furman et al., 2019). Previously, we were using a colonic carcinoma cell line (Caco-2) and observed a downregulation of *COX-2*, *TNF-α, iNOS, ICAM-1*, and *NFκB* expression in response to TF-2 (Gosslau et al., 2011a; Lu et al., 2000). Here, we used Caco-2 cells to look for effects of BZ-6 (50 µg/mL) on TPA-induced *COX-2* expression (Figure 5c). After 3 hours we observed a significant attenuation of *COX-2* as demonstrated by conventional RT-PCR ($P < 0.05$). Our observation might be interesting in the context of several reports of anti-cancer, anti-proliferative and proapoptotic effects described for purpurogallin (Abou-Karam and Shier, 1999; Chakrabarty et al., 2013; Kitada et al., 2003; Watanabe et al., 2009). These results might further strengthen the hypothesis that the benzotropolone core structure plays an important role in the anti-cancer potential of anti-inflammatory black tea polyphenols.

## 4. Discussion

Black tea has well-documented health beneficial and therapeutic effects against a variety of degenerative diseases. It is generally believed that the health-promoting effects of black tea are based on anti-oxidant and anti-inflammatory activities of the three theaflavin isoforms as major bioactives (Du et al., 2025; He, 2017; Li et al., 2013; Samanta, 2022; Sang et al., 2011). In accordance to its anti-inflammatory effects several studies demonstrated effects of black tea against diseases related to chronic inflammation such as cardiovascular, gastrointestinal, neurological and immunological disorders, diabetes, rheumatoid arthritis and different cancers (Du et al., 2025; Li et al., 2013; Samanta, 2022; Sang et al., 2011). In addition, pro-apoptotic activities of theaflavins are attributed to anti-cancer effects (Du et al., 2025; Gao et al., 2013; Gosslau et al., 2011a; Samanta, 2022; Tu et al., 2016). The benzotropolone moiety as the core structure of theaflavins raised our interest for a mechanistic SAR study analyzing anti-proliferative as well as anti-inflammatory bioactivities using nine BZ derivatives. Importantly, a comparison throughout low molecular derivatives demonstrated that positioning of functional groups around the benzotropolone core structure dramatically affected the biological activity against proliferation and inflammation: BZ-6 representing the benzotropolone core moiety showed both strong anti-proliferative and anti-inflammatory effects. ntriguingly, BZ-6 showed comparable anti-inflammatory effects to ibuprofen in our paw edema animal model. Recently, we demonstrated that ibuprofen as widely accepted NSAIDs showed also effects against type 2 diabetes (Gosslau et al., 2024; Rainsford, 2009). The addition of either a hydroxyl group at C-2 (BZ-5) or carboxyl group at C-1 (BZ-7), respectively, resulted in relative mild anti-proliferative effects, whereas strong anti-inflammatory activities appeared to be unchanged. Noteworthy, the new compound BZ-7 showed strongest anti-inflammatory activity with least cytotoxic effects. On the other hand, the addition of a carboxyl group at C-8 (BZ-8) induced a low anti-inflammatory activity and relative mild anti-proliferative effects. The derivative with two additional carboxyl groups at C-1 and C-8 (BZ-9) exhibited lowest anti-proliferative and no anti-inflammatory bioactivity as judged by COX-2 expression (Figure 3). These features are in correspondence to earlier studies suggesting specific cellular sites serving as pharmacological targets of benzotropolones (Gosslau et al., 2018; Sang et al., 2011; Sang et al., 2004). Previously, we observed a suppression of *c-Jun* and *c-Fos* in a skin inflammation

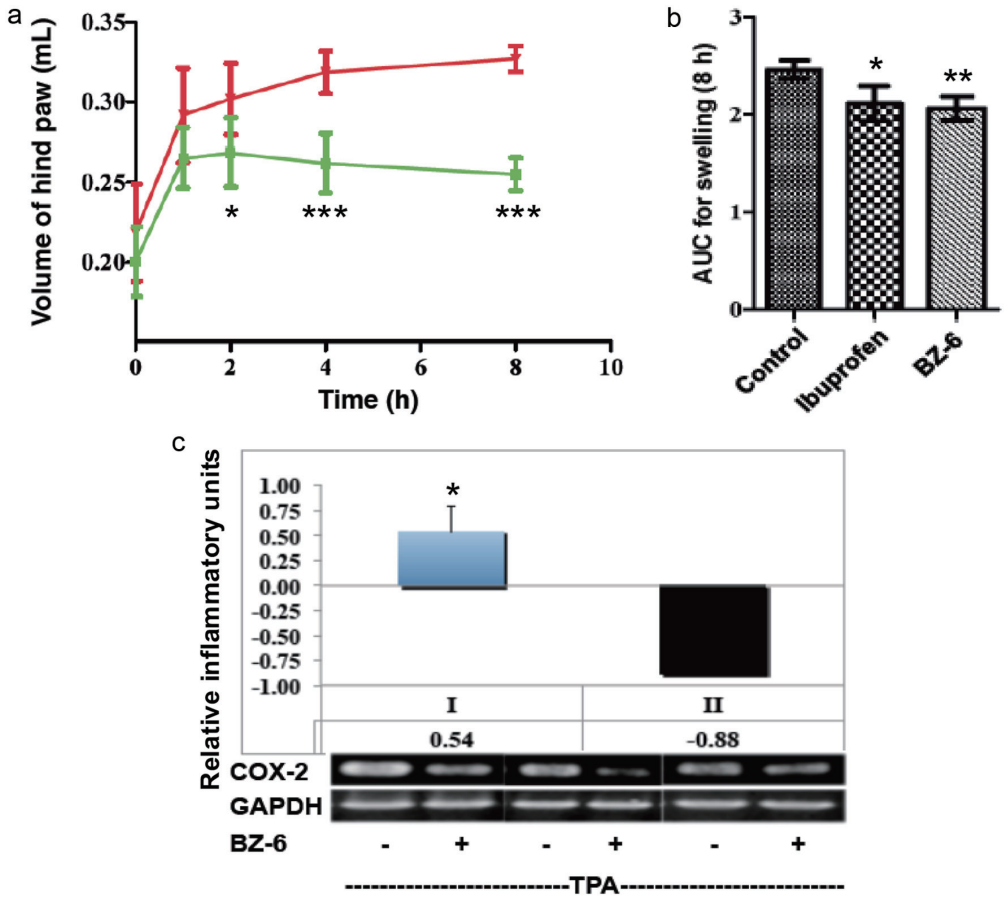


**Figure 5. Effects of BZ-6 on carrageenan-induced paw edema in mice and in Caco-2 cells.** (a, b) Mice received a single oral dose of control vehicle (tocopherol-stripped corn-oil), BZ-6 (250 mg/kg), or ibuprofen (100 mg/kg), respectively. 1 h after treatment, all groups received an injection of 0.1 mL of carrageenan (1% in water) into the plantar side of the right hind paw (n = 6 for each group per time point). The mice were then euthanized 1, 2, 4, and 8 h after carrageenan injection. The degree of swelling was determined by paw volume displacement measured at indicated times by a digital hydroplethysmometer. Results are expressed as mean ± SD of the volume of hind paw (mL) for different time points (a) or as area under the curve (AUC) units after 8 h (b), respectively. (c) Human colorectal carcinoma cells (Caco-2) were treated with TPA (20nM) either alone or in combination with BZ-6 (50 µg/ml) for 3h. After RNA isolation and reverse transcription, gene expression of *COX-2* and *GAPDH* was analyzed by RT-PCR and quantified using densitometry. *COX-2* expression normalized to *GAPDH* is expressed either as ratio of the mean experimental channel (TPA + BZ) to the mean control channel (TPA alone) ± standard deviation (I) or inflammatory index (II), respectively. Mean values + standard deviation of three independent experiments with representative blots are shown in the histograms. *, **, and *** indicate significant differences from the control group with $P < 0.05$, 0.01 or 0.001, respectively as analyzed by ANOVA (a, b) or students *t*-test (c).

model and a *COX-2* promoter reporter assay confirming a role of NFκB and AP-1 in the anti-inflammatory effects of TF-2 (Gosslau et al., 2011a).

A mystery in tea research has been the discrepancy between the well-established bioactivity of high molecular weight theaflavins on the one hand and poor bioavailability on the other (Li et al., 2025; Sang et al., 2011; Shi et al., 2022; Takeda et al., 2013). This is evident either by the failure or detection of only minute amounts of theaflavins in blood or urine as demonstrated by *in vivo* animal and clinical settings (Chen et al., 2011; Henning et al., 2006; Li et al., 2025; Mulder et al., 2001; Sang et al., 2011; Shi et al., 2022). Due to the recent understanding of the important role of microbiota in nutrition biotransformation of black tea polyphenols metabolized by gut microbiota are discussed to play an important role in their health benefits. For theaflavins, surprisingly little research on absorption and microbial metabolism had been conducted and so far, no small BZ compounds had been detected in blood or urine (Gosslau et al., 2018).

In several studies it have been demonstrated that natural occurring PPG (2,3,4,5-tetrahydroxybenzo[7]annulen-6-one) induced a downregulation of a variety of inflammatory genes such *COX*-2, *TNF-α*, *ICAM-1*, *iNOS*, *IL-1β* and *IL-6* (Chang et al., 2014; Kim et al., 2011; Park et al., 2013) in correspondence to our results. Mechanistic studies point to an interaction of PPG targeting inflammatory pathways such as NFκB, 3-kinase/Akt and/or mitogen-activated protein kinase signaling pathways (Chang et al., 2014; Kim et al., 2011; Park et al., 2013). For the NFκB signaling cascade, a suppression of the translocation of the p65 NFκB subunit into the nucleus and the degradation of IκB had been shown to be the molecular mechanisms leading to attenuation of inflammation (Park et al., 2013). Interestingly, we observed only a minor attenuation of the p65 subunit of *NFκB* in our gene expression analysis by BZ-5, BZ-6, BZ-7 and also BZ-8 which correlate to a regulation mainly on posttranslational level to initiate the induction of many key inflammatory genes (Aggarwal et al., 2012; Baud and Karin, 2009; Furman et al., 2019; Ghosh and Hayden, 2008;

Robbins et al., 2010; van de Vyver, 2023). Since we observed a similar pattern in the downregulation of inflammatory genes for BZ-6 and BZ-7 as compared to PPG, a post-translational regulation of NFκB by these compounds might be postulated. Interestingly, although at high concentrations, BZ-6 induced a decrease in *c-Jun* and *c-Fos* expression suggesting an additional role of AP-1 for anti-inflammatory effects at least of BZ-6. Activator protein-1 (AP-1) represents another transcription factor controlling many inflammatory genes by different compositions of homodimers and/or heterodimers of the Jun, Fos, activating transcription factor (ATF), and musculoaponeurotic fibrosarcoma (MAF) protein families (Shaulian and Karin, 2002; Zenz et al., 2008).

The importance of apoptosis in chemoprevention or chemotherapy is apparent, as a defect in apoptotic mechanisms is recognized as an important cause of carcinogenesis (Reed, 2003). The induction of apoptosis has been described for TF-1, TF-2 and TF-3 (Du et al., 2025; Gao et al., 2013; Gosslau et al., 2011a; Samanta, 2022; Tu et al., 2016) which correlate to prominent effects of black tea against different types of cancer. Since proapoptotic effects for purpurogallin have been reported (Abou-Karam and Shier, 1999; Chakrabarty et al., 2013; Kitada et al., 2003; Watanabe et al., 2009) it is likely that induction of apoptotic cell death might be the mode of action for at least some of the other derivatives which showed strong anti-proliferative effects (e.g. BZ-6). Previously, we used human colonic carcinoma cells (Caco-2) in addition to two mouse models for inflammation and observed a downregulation of TPA-induced *COX-2*, *TNF-α, iNOS, ICAM-1*, and *NFκB* expression in response to TF-2 (Gosslau et al., 2011a; Lu et al., 2000). Our observation of a significant downregulation of *COX-2* in Caco-2 cells but also anti-proliferative effects against U-937 cells are in line with reports of anti-cancer effects of PPG (Abou-Karam and Shier, 1999; Chakrabarty et al., 2013; Kitada et al., 2003; Watanabe et al., 2009) but also some other benzotropolone derivatives (Sang et al., 2004). A dose response analysis performed with BZ-6 showed strong anti-inflammatory effects at low concentrations (e.g. 25 µM; see Figure 4a) in U-937 cells and we can only speculate on effective concentrations in the lower range of BZ-6 but also the other small benzotropolone derivatives. We can also only hypothesize on the underlying mechanisms of the divergent anti-proliferative effects as measured by the MTT which usually correlates to cytotoxic effects as measured by trypan blue or other dye exclusion assays (data not shown) and the anti-inflammatory activity. It appears that the three most relevant BZs (e.g., BZ-5, -6 and -7) showed a similar pattern in the downregulation of inflammatory biomarkers (e.g., *COX-2*, *TNF-α*, *ICAM-1*, *NFκB*, *IL-1β*, and *IL-8*) with strongest effects for BZ-7 on the one hand and least cytotoxic effects on the other. Therefore, it may be hypothesized that other cytokines show a different display in response to these BZs thus inducing a differential cytokine storm translating into different cytotoxicity (Nie et al., 2025).

## 5. Conclusion

Our study substantiated former studies showing strong anti-inflammatory bioactivities of the natural occurring benzotropolone (e.g. purpurogallin) but also some other new derivatives. Importantly, the positioning of functional groups around the benzotropolone moiety are crucial for anti-proliferative and anti-inflammatory activities. Intriguingly, the benzotropolone moiety exhibited strong effects against inflammation comparable to ibuprofen in the paw edema model. Information gained by our group but also elsewhere indicate that anti-inflammatory effects of BZs are based on specific interaction either directly or indirectly leading to attenuation majorly of NFκB signaling but also MAPK and/or AP-1 pathways. The accumulating evidence of strong bioactivities exhibited by benzotropolones might pinpoint to their role as potential metabolites to resolve the discrepancy between strong bioactivity and poor bioavailability of tea polyphenols. Biotransformation by biodiverse gut microbiota in response to different nutrition might be of particular importance (Gosslau et al., 2018). So far *in vivo* detection of BZ derivatives in urine or blood is warranted. Further mechanistic studies on bioavailability, bioaccessibility and bioactivity are needed to consolidate the role of BZs as bioactive metabolites of black tea providing the foundation for potential therapeutic applications. Particularly, the effects of bioactive BZ compounds exhibiting only mild toxicity such as BZ-7 and PPG are very promising. Although still very preliminary these reports further emphasize the potential of benzotropolones against diseases associated with chronic inflammation which needs to be substantiated by further clinical studies.

## Acknowledgments

The authors wish to thank WellGen Inc. for support of materials.

## References

Abou-Karam, M., and Thomas Shier, W. (1999). Inhibition of oncogene product enzyme activity as an approach to cancer chemoprevention. Tyrosine-specific protein kinase inhibition by purpurogallin fromQuercus sp. Nutgall. Phytother. Res. 13: 337–340.

Aggarwal, B.B., Krishnan, S., and Guha, S. (2012). Inflammation, Lifestyle and Chronic Diseases: The Silent Link (Oxidative Stress and Disease). CRC Press, Boca Raton.

Baud, V., and Karin, M. (2009). Is NF-κB a good target for cancer therapy? Hopes and pitfalls. Nature Reviews Drug Discov. 8: 33–40.

Berg, K., Hansen, M., and Nielsen, S. (1990). A new sensitive bioassay for precise quantification of interferon activity as measured via the mitochondrial dehydrogenase function in cells (MTT-method). APMIS 98: 156–162.

Bernhard, D., Schwaiger, W., Crazzolara, R., Tinhofer, I., Kofler, R., and Csordas, A. (2003). Enhanced MTT-reducing activity under growth inhibition by resveratrol in CEM-C7H2 lymphocytic leukemia cells. Cancer Lett. 195: 193–199.

Calle, M.C., and Fernandez, M.L. (2012). Inflammation and type 2 diabetes. Diabetes Metab. 38: 183–191.

Chakrabarty, S., Croft, M.S., Marko, M.G., and Moyna, G. (2013). Synthesis and evaluation as potential anticancer agents of novel tetracyclic indenoquinoline derivatives. Bioorg Med. Chem. 21: 1143–1149.

Chang, C.Z., Lin, C.L., Wu, S.C., and Kwan, A.L. (2014). Purpurogallin, a natural phenol, attenuates high-mobility group box 1 in subarachnoid hemorrhage induced vasospasm in a rat model. Int. J. Vasc. Med. 2014: 254270.

Chaudhary, M.R., Chaudhary, S., Sharma, Y., Singh, T.A., Mishra, A.K., Sharma, S., and Mehdi, M.M. (2023). Aging, oxidative stress and degenerative diseases: mechanisms, complications and emerging therapeutic strategies. Biogerontology 24: 609–662.

Chen, H., Parks, T.A., Chen, X., Gillitt, N.D., Jobin, C., and Sang, S. (2011). Structural identification of mouse fecal metabolites of theaflavin 3,3'-digallate using liquid chromatography tandem mass spectrometry. J. Chromatogr. A 1218: 7297–7306.

Coussens, L.M., and Werb, Z. (2002). Inflammation and cancer. Nature 420: 860–867.

Davies, K. (1995). Oxidative stress: the paradox of aerobic life. Portland Press, London, pp. 1–31.

Drynan, J.W., Clifford, M.N., Obuchowicz, J., and Kuhnert, N. (2010). The chemistry of low molecular weight black tea polyphenols. Nat. Prod.

Rep. 27: 417–462.
Du, S., Chang, J., and Zhou, Z. (2025). A Comprehensive Review of Theaflavins: Physiological Activities, Synthesis Techniques, and Future Challenges. Food Sci. Nutr. 13: e70762.
Forsbeck, K., Nilsson, K., Hansson, A., Skoglund, G., and Ingelman-Sundberg, M. (1985). Phorbol ester-induced alteration of differentiation and proliferation in human hematopoietic tumor cell lines: relationship to the presence and subcellular distribution of protein kinase C. Cancer Res 45: 6194–6199.
Furman, D., Campisi, J., Verdin, E., Carrera-Bastos, P., Targ, S., Franceschi, C., Ferrucci, L., Gilroy, D.W., Fasano, A., Miller, G.W., Miller, A.H., Mantovani, A., Weyand, C.M., Barzilai, N., Goronzy, J.J., Rando, T.A., Effros, R.B., Lucia, A., Kleinstreuer, N., and Slavich, G.M. (2019). Chronic inflammation in the etiology of disease across the life span. Nat. Med. 25: 1822–1832.
Gao, Y., Li, W., Jia, L., Li, B., Chen, Y.C., and Tu, Y. (2013). Enhancement of (-)-epigallocatechin-3-gallate and theaflavin-3-3'-digallate induced apoptosis by ascorbic acid in human lung adenocarcinoma SPC-A-1 cells and esophageal carcinoma Eca-109 cells via MAPK pathways. Biochem. Biophys. Res. Commun. 438: 370–374.
Ghosh, S., and Hayden, M.S. (2008). New regulators of NF-kappaB in inflammation. Nat. Rev. Immunol. 8: 837–848.
Gosslau, A., Chen, K.Y., Ho, C.-T., and Li, S. (2014). Anti-inflammatory effects of characterized orange peel extracts enriched with bioactive polymethoxyflavones. Food Sci. Human Wellness 3: 26–35.
Gosslau, A., En Jao, D.L., Huang, M.T., Ho, C.T., Evans, D., Rawson, N.E., and Chen, K.Y. (2011a). Effects of the black tea polyphenol theaflavin-2 on apoptotic and inflammatory pathways in vitro and in vivo. Mol. Nutr. Food. Res. 55: 198–208.
Gosslau, A., Li, S., Ho, C.T., Chen, K.Y., and Rawson, N.E. (2011b). The importance of natural product characterization in studies of their anti-inflammatory activity. Mol. Nutr. Food Res. 55: 74–82.
Gosslau, A., Li, S., Zachariah, E., and Ho, C.-T. (2018). Therapeutic Connection Between Black Tea Theaflavins and Their Benzotropolone Core Structure. Curr. Pharmacol. Rep. 4: 447–452.
Gosslau, A., Sisk, S., Huang, M.-T., Ho, C.-T., and Chen, K.Y. (2008). P7 - Case study of an anti-inflammatory ingredient discovered via nutrigenomic screening. J. Nutrigenet. Nutrigenomics. 1: 76–77.
Gosslau, A., Ozdogru, U., Zachariah, E., Li, S., and Ho, C.-T. (2024). Effects of ibuprofen in the ZDF rat model of type 2 diabetes. J. Food Drug Anal. 32: 227–238.
He, H.F. (2017). Research progress on theaflavins: efficacy, formation, and preparation. Food Nutr Res. 61: 1344521.
Henning, S.M., Aronson, W., Niu, Y., Conde, F., Lee, N.H., Seeram, N.P., Lee, R.P., Lu, J., Harris, D.M., Moro, A., Hong, J., Pak-Shan, L., Barnard, R.J., Ziaee, H.G., Csathy, G., Go, V.L., Wang, H., and Heber, D. (2006). Tea polyphenols and theaflavins are present in prostate tissue of humans and mice after green and black tea consumption. J. Nutr. 136: 1839–1843.
Ho, C.-T., Ghai, G., Sang, S., Jhou, J.-W., Huang, M.-T., Rosen, R.T., and Dushenkov, S. (2006). Benzotropolone derivatives and modulation of inflammatory response. Vol. US 7087790. U.S. Patent, editor, United States of America.
Ho, C.-T., Lin, J.-K., and Shahidi, F. (2008). Tea and Tea Products: Chemistry and Health-Promoting Effects.. CRC Press, Taylor & Francis Group, Boca Raton, Florida.
Kim, T.H., Ku, S.-K., Lee, I.-C., and Bae, J.-S. (2011). Anti-inflammatory functions of purpurogallin in LPS-activated human endothelial cells. BMB Rep. 45(3): 200–205.
Kitada, S., Leone, M., Sareth, S., Zhai, D., Reed, J.C., and Pellecchia, M. (2003). Discovery, characterization, and structure-activity relationships studies of proapoptotic polyphenols targeting B-cell lymphocyte/leukemia-2 proteins. J. Med. Chem. 46: 4259–4264.
Ley, K. (2001). Physiology of Inflammation. Oxford University Press, New York.
Li, M., Li, W., Dong, Y., Zhan, C., Tao, T., Kang, M., Zhang, C., and Liu, Z. (2025). Advances in metabolism pathways of theaflavins: digestion, absorption, distribution and degradation. Crit. Rev. Food Sci. Nutr. 65: 4195–4203.
Li, S., Lo, C.Y., Pan, M.H., Lai, C.S., and Ho, C.T. (2013). Black tea: chemical analysis and stability. Food Funct. 4: 10–18.
Lu, J., Ho, C.T., Ghai, G., and Chen, K.Y. (2000). Differential effects of theaflavin monogallates on cell growth, apoptosis, and Cox-2 gene expression in cancerous versus normal cells. Cancer Res. 60: 6465–6471.
Maldonado, E., Morales-Pison, S., Urbina, F., and Solari, A. (2023). Aging Hallmarks and the Role of Oxidative Stress. Antioxidants (Basel) 12: 651.
Moilanen, L.J., Laavola, M., Kukkonen, M., Korhonen, R., Leppanen, T., Hogestatt, E.D., Zygmunt, P.M., Nieminen, R.M., and Moilanen, E. (2012). TRPA1 contributes to the acute inflammatory response and mediates carrageenan-induced paw edema in the mouse. Sci. Rep. 2: 380.
Morris, C.J. (2003). Carrageenan-induced paw edema in the rat and mouse. Methods Mol. Biol. 225: 115–121.
Mulder, T.P., van Platerink, C.J., Wijnand Schuyl, P.J., and van Amelsvoort, J.M. (2001). Analysis of theaflavins in biological fluids using liquid chromatography-electrospray mass spectrometry. J. Chromatogr. B Biomed. Sci. Appl. 760: 271–279.
Nie, J., Zhou, L., Tian, W., Liu, X., Yang, L., Yang, X., Zhang, Y., Wei, S., Wang, D.W., and Wei, J. (2025). Deep insight into cytokine storm: from pathogenesis to treatment. Signal Transduct. Target. Ther. 10: 112.
Park, H.Y., Kim, T.H., Kim, C.G., Kim, G.Y., Kim, C.M., Kim, N.D., Kim, B.W., Hwang, H.J., and Choi, Y.H. (2013). Purpurogallin exerts anti?inflammatory effects in lipopolysaccharide?stimulated BV2 microglial cells through the inactivation of the NF?kappaB and MAPK signaling pathways. Int. J. Mol. Med. 32: 1171–1178.
Prasad, K., Kapoor, R., and Lee, P. (1994). Purpurogallin, a scavenger of polymorphonuclear leukocyte-derived oxyradicals. Mol. Cell. Biochem. 139: 27–32.
Rainsford, K.D. (2009). Ibuprofen: pharmacology, efficacy and safety. Inflammopharmacol. 17: 275–342.
Reed, J.C. (2003). Apoptosis-targeted therapies for cancer. Cancer Cell. 3: 17–22.
Robbins, S.L., Kumar, V., and Cotran, R.S. (2010). Pathologic basis of disease, Chapter 2: Acute and chronic Inflammation. Elsevier Saunders, Philadelphia.
Samanta, S. (2022). Potential Bioactive Components and Health Promotional Benefits of Tea (Camellia sinensis). J. Am. Nutr. Assoc. 41: 65–93.
Sang, S., Lambert, J.D., Ho, C.T., and Yang, C.S. (2011). The chemistry and biotransformation of tea constituents. Pharmacol. Res. 64: 87–99.
Sang, S., Lambert, J.D., Tian, S., Hong, J., Hou, Z., Ryu, J.H., Stark, R.E., Rosen, R.T., Huang, M.T., Yang, C.S., and Ho, C.T. (2004). Enzymatic synthesis of tea theaflavin derivatives and their anti-inflammatory and cytotoxic activities. Bioorg. Med. Chem. 12: 459–467.
Shaulian, E., and Karin, M. (2002). AP-1 as a regulator of cell life and death. Nat. Cell. Biol. 4: E131–136.
Shi, M., Lu, Y., Wu, J., Zheng, Z., Lv, C., Ye, J., Qin, S., and Zeng, C. (2022). Beneficial Effects of Theaflavins on Metabolic Syndrome: From Molecular Evidence to Gut Microbiome. Int. J. Mol. Sci. 23: 7595.
Smith, W.L., DeWitt, D.L., and Garavito, R.M. (2000). Cyclooxygenases: structural, cellular, and molecular biology. Annu. Rev. Biochem. 69: 145–182.
Takeda, J., Park, H.Y., Kunitake, Y., Yoshiura, K., and Matsui, T. (2013). Theaflavins, dimeric catechins, inhibit peptide transport across Caco-2 cell monolayers via down-regulation of AMP-activated protein kinase-mediated peptide transporter PEPT1. Food Chem. 138: 2140–2145.
Tanaka, T., and Matsuo, Y. (2020). Production Mechanisms of Black Tea Polyphenols. Chem. Pharm. Bull. (Tokyo) 68: 1131–1142.
Tu, Y., Kim, E., Gao, Y., Rankin, G.O., Li, B., and Chen, Y.C. (2016). Theaflavin-3, 3'-digallate induces apoptosis and G2 cell cycle arrest through the Akt/MDM2/p53 pathway in cisplatin-resistant ovarian cancer A2780/CP70 cells. Int. J. Oncol. 48: 2657–2665.
van de Vyver, M. (2023). Immunology of chronic low-grade inflammation: relationship with metabolic function. J. Endocrinol. 257: e220271.
Watanabe, N., Sekine, T., Takagi, M., Iwasaki, J., Imamoto, N., Kawasaki, H., and Osada, H. (2009). Deficiency in chromosome congression by the inhibition of Plk1 polo box domain-dependent recognition. J. Biol. Chem. 284: 2344–2353.
Wu, Y., Jin, F., Wang, Y., Li, F., Wang, L., Wang, Q., Ren, Z., and Wang, Y. (2016). In vitro and in vivo anti-inflammatory effects of theaflavin-3,3'-digallate on lipopolysaccharide-induced inflammation. Eur. J.

Pharmacol. 794: 52–60.
Wu, T.W., Wu, J., Zeng, L.H., Au, J.X., Carey, D., and Fung, K.P. (1994). Purpurogallin: in vivo evidence of a novel and effective cardioprotector. Life Sci. 54: PL23–28.
Wu, T.W., Zeng, L.H., Wu, J., and Carey, D. (1991). Purpurogallin--a natural and effective hepatoprotector in vitro and in vivo. Biochem. Cell. Biol. 69: 747–750.
Wu, T.W., Zeng, L.H., Wu, J., Fung, K.P., Weisel, R.D., Hempel, A., and Camerman, N. (1996). Molecular structure and antioxidant specificity of purpurogallin in three types of human cardiovascular cells. Biochem. Pharmacol. 52: 1073–1080.
Wu, Y., Jin, F., Wang, Y., Li, F., Wang, L., Wang, Q., Ren, Z., and Wang, Y. (2017). In vitro and in vivo anti-inflammatory effects of theaflavin-3,3'-digallate on lipopolysaccharide-induced inflammation. Eur. J. Pharmacol. 794: 52–60.
Zeng, L.H., and Wu, T.W. (1992). Purpurogallin is a more powerful protector of kidney cells than Trolox and allopurinol. Biochem. Cell. Biol. 70: 684–690.
Zenz, R., Eferl, R., Scheinecker, C., Redlich, K., Smolen, J., Schonthaler, H.B., Kenner, L., Tschachler, E., and Wagner, E.F. (2008). Activator protein 1 (Fos/Jun) functions in inflammatory bone and skin disease. Arthritis. Res. Ther. 10: 201.